Fatigue Crack Growth Modelling in Welded Stiffened Panels under Cyclic Tension

Željko Božić[1,*], Siegfried Schmauder[2], Marijo Mlikota[2], Martin Hummel[2]

[1] University of Zagreb, Faculty of Mech. Eng. And Nav. Arch., I. Lucica 5, 10000 Zagreb, Croatia
[2] University of Stuttgart, IMWF, Pfaffenwaldring 32, D-70569 Stuttgart
* Corresponding author: zeljko.bozic@fsb.hr

Abstract The influence of welding residual stresses in stiffened panels on effective stress intensity factor values and fatigue crack growth rate was studied in this paper. Interpretation of relevant effects on different length scales such as dislocation appearance and microstructural crack nucleation and propagation are taken into account using Molecular Dynamics (MD) simulations as well as a Tanaka-Mura approach for the analysis of the problem. Mode I stress intensity factors (SIF), K_I, were calculated by the ANSYS program using shell elements and assuming plane stress conditions. The SIFs were calculated from FE results using the crack tip displacement extrapolation method. A total SIF value, K_{tot}, is contributed by the part due to the applied load K_{app}, and by the part due to weld residual stresses, K_{res}. In the FE software package ANSYS the command INISTATE is used for defining the initial stress conditions. The FE analysis for the stiffened panel specimens showed that high tensile residual stresses in the vicinity of a stiffener significantly increase K_{res} and K_{tot}. Correspondingly, the simulated crack growth rate was higher in this region, which is in good agreement with experimental results. Compressive weld residual stresses between two stiffeners decreased the effective SIF value, K_{eff}, which was considered as a crack growth driving force in a power law model.

Keywords Fatigue crack growth rate, Welding residual stresses, Stiffened panel, Dislocation, Microstructural crack

1. Introduction

In stiffened panels of a ship deck structure, fatigue cracks may initiate under cyclic loading at sites of stress concentration and further propagate, which can eventually result in unstable fracture and structural failure. The crack growth rate in welded stiffened panels can be significantly affected by the residual stresses which are introduced by the welding process. The high heat input from the welding process causes tensile residual stresses in the vicinity of a stiffener. These tensile stresses are equilibrated by compressive stresses in the region between the stiffeners. Welding residual stresses should be taken into account for a proper fatigue life assessment of welded stiffened panels under cyclic tension loading.

The complete process of fatigue failure of mechanical components may be divided into the following stages: (1) micro-crack nucleation; (2) small crack growth; (3) long crack growth; and (4) occurrence of final failure. In engineering applications, the first two stages are usually termed as the "crack initiation or small crack formation period" while long crack growth is termed as the ''crack propagation period". Dislocation development can be simulated by using the molecular dynamics (MD) simulation code IMD [1]. To analyze dislocation development atomistic scale simulation methods are implemented, [2, 3, 4, 5].

The crack initiation period generally accounts for most of the service life, especially in high-cycle and very high cycle fatigue [6]. In pure metals and some alloys without pores or inclusions, irreversible dislocations glide under cyclic loading. This leads to the development of persistent slip bands, extrusions and intrusions in surface grains that are optimally oriented for slip. With continued strain cycling, a fatigue crack can be nucleated at an extrusion or intrusion within a

persistent slip band. [7, 8, 9, 10, 11, 12, 13].
Non-metallic inclusions, which are present in commercial materials as a result of the production process, can also act as potential sites for fatigue crack nucleation. In the high cycle regime fatigue cracks initiate from inclusions and defects on the surface of a specimen or component. For very high cycle fatigue, fatigue cracks initiate from defects located under the surface of the specimen [14,15]. Micro-crack nucleation can be analyzed by using the Tanaka-Mura model or some of its modifications [16, 17, 18].
Fatigue crack growth prediction models based on fracture mechanics have been developed to support the damage tolerance concepts in metallic structures, [19]. A well known method for predicting fatigue crack propagation under constant stress range is a power law described by Paris and Erdogan [20]. Dexter et al. [21, 22] analysed the growth of long fatigue cracks in stiffened panels and simulated the crack propagation in box girders with welded stiffeners. He conducted cyclic tension fatigue tests on approximately half-scale welded stiffened panels to study propagation of large cracks as they interact with the stiffeners. Measured welding residual stresses were introduced in the finite element model and crack propagation life was simulated. Sumi at al. [23] studied the fatigue growth of long cracks in stiffened panels of a ship deck structure under cyclic tension loading. For that purpose fatigue tests were carried out on welded stiffened panel specimens damaged with a single crack or an array of collinear cracks.
This paper presents a study of the influence of welding residual stresses in stiffened panels on effective stress intensity factor values and fatigue crack growth rate. Mode I SIF values, K_I, were calculated by the FE software package ANSYS using shell elements and the crack tip displacement extrapolation method in an automatic post processing procedure. A total SIF value, K_{tot}, was obtained by a linear superposition of the SIF values due to the applied load, K_{app}, and due to weld residual stresses, K_{res}. The effective SIF value, K_{eff}, as defined by Elber [24], was considered as a crack growth driving force in a power law model. Simulated fatigue crack propagation life was compared with the experimental results as obtained by Sumi at al. [23]. The molecular dynamics (MD) simulation was implemented to analyze dislocation development in an iron cuboid model with a triangular notch tip. Numerical simulations of the fatigue crack initiation and growth for martensitic steel, based on modified Tanaka-Mura, were carried out.

2. Molecular dynamics (MD) simulation of dislocation development in iron

2.1. Methods and model

Taking a close look on dislocation development leads to the necessity of atomistic scale simulation methods. Therefore, we used for the present work the molecular dynamics (MD) simulation code IMD [1]. It was developed at the Institute of Theoretical and Applied Physics (ITAP) belonging to the University of Stuttgart. In MD the atoms are seen as mass m points at the position $\vec{r}$ for which Newton´s equations of motion:

$$F(\vec{r},t) = m * \frac{\partial^2 \vec{r}}{\partial^2 t} \tag{1}$$

are solved in every time step. The force $F(\vec{r},t)$ is given by the derivative of the interatomic embedded atom method (EAM) [2] pair potential $U(\vec{r},t)$ (Eq. 2):

$$F(\vec{r},t) = -\nabla U(\vec{r},t) \tag{2}$$

The system we investigated contains about half a million iron atoms. They form a cuboid of the size

286 x 143 x 143 Å³ where a notch (dimensions 15 x 90 Å²) with a triangular notch tip was inserted along the (110) plane.

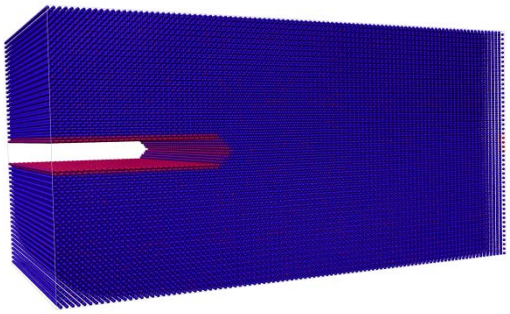

Figure 1. Bcc iron cuboid 286 x 143 x 143 Å³ with a 15 x 90 Å² notch on a (110) plane. The 486000 atoms are color coded via von Mises stress (red ≙ high stress, blue ≙ low stress). Image by MegaMol™ [3].

Cyclic deformation of the simulation box was applied in the [001]-direction. Therefore, the z-component of the simulation cell was elongated with a constant rate of 5x10^-7 at each time step. After reaching a strain of seven percent we applied pressure at the same rate until we reach seven percent of strain in compression. This procedure was repeated continuously. Periodic boundary conditions were used in every direction.

2.2. Results and discussion

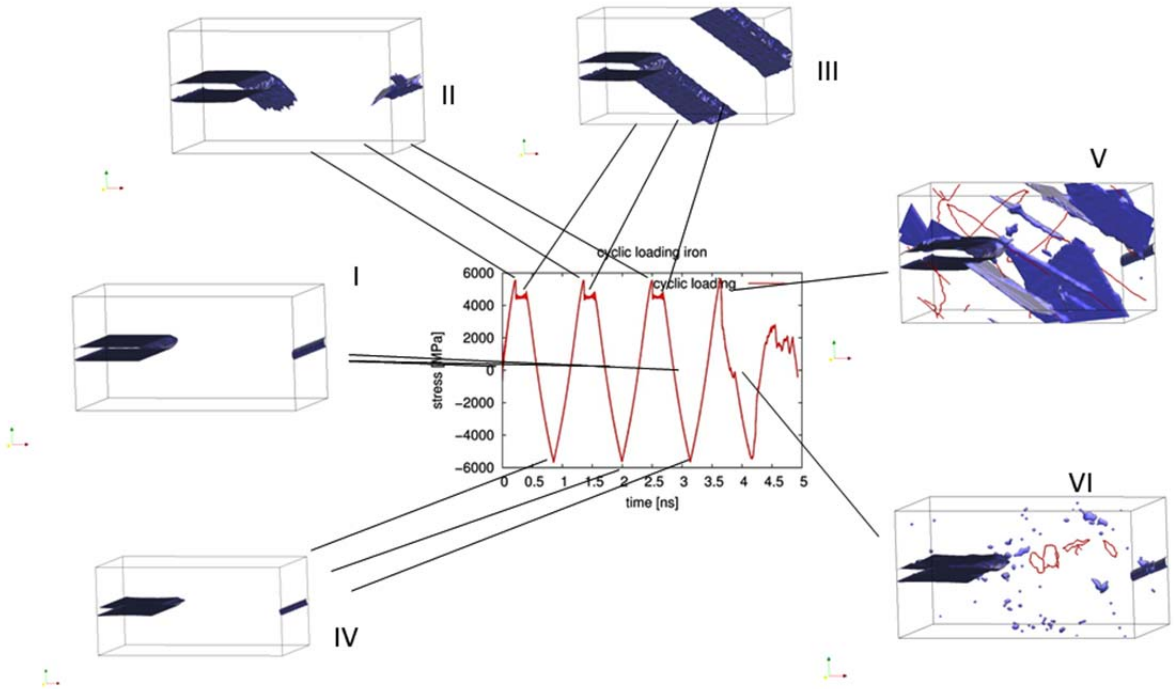

Figure 2. Stress [MPa] in z-direction in terms of the time [ns] during cyclic loading of a nanostructure of a notched iron cuboid. System configurations at different times are depicted: blue are according to DXA [4] "defect surfaces", red represent dislocations. The view is from lower left.

During the continuous cyclic change from elongation to compression different stages of the system appeared (see Figure 2).

- Stage I: Configuration under no pressure.
- Stage II: Initiation of reversible local restructuring under tensile loading.
- Stage III: Formation of one continuous plane with hcp structure.
- Stage IV: Compression leads to a resolution of the deformation introduced in the previous steps into the structure and to bending of the middle of the notch surfaces towards each other up to a minimum distance of 6.8 Å.
- Stage V: During the fourth loading cycle dislocations are initiated. The Dislocation Extraction Algorithm (DXA) [4] detects "defect surfaces". "The defect surface consists of those parts of the interface mesh, which have not been swept by elastic Burgers circuits." [5]
- Stage VI: Dislocations still remain in the structure even though no pressure remains in the system.

3. Microstructural crack nucleation and propagation

To solve problems of micro-crack nucleation the Tanaka-Mura model [16] is frequently used. The number of stress cycles N_c required for micro-crack nucleation can be determined as follows:

$$N_c = \frac{8GW_s}{\pi(1-\nu)d(\Delta\bar{\tau}-2k)^2} \tag{3}$$

Eq. (3) presumes that micro-cracks form along slip bands within grains, depending on slip band length d and average shear stress range $\Delta\bar{\tau}$ on the slip band. Other material constants (shear modulus G, specific fracture energy per unit area W_s, Poisson's ratio ν and frictional stress of dislocations on the slip plane can be found in the specialized literature [17]. Jezernik et al. [18] used the Tanaka-Mura model to numerically simulate the small crack formation process. Three improvements were added to this model: (a) multiple slip bands inside each crystal grain as potential sites for crack nucleation, (b) micro-crack coalescence between two grains and (c) segmented micro-crack generation inside one grain. A numerical model was directed at simulating fatigue properties of thermally cut steel. The authors took into account accompanying residual stresses in order to simulate the properties of the thermally cut edge as faithfully as possible.

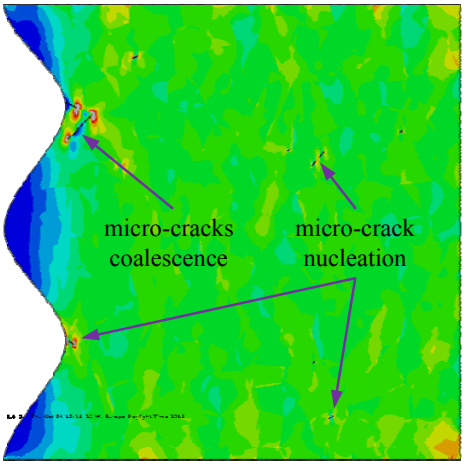

Figure 3. Micro-crack nucleation and subsequent coalescence [18]

As residual stresses are not considered in the Tanaka-Mura model according to Eq. (3), they are imposed as additional external loading. Therefore, the residual stresses are in the Tanaka-Mura equation implicitly evaluated through the average shear stress range on the slip band $\Delta\bar{\tau}$. Figure 3 shows the shear stress distribution and nucleated micro-cracks for a typical high cycle fatigue regime load level (450 MPa). In the beginning, micro-cracks tended to occur scattered in the model and form in larger grains that are favorably oriented and show higher shear stresses. But after a while, existing micro-cracks started coalescing, causing local stress concentrations and amplifying the likelihood of new micro-cracks forming near already coalesced cracks.

4. Modeling and analysis of crack propagation in welded stiffened panels

It is well-known that the residual stress in a welded stiffened panel is tensile along a welded stiffener and compressive in between the stiffeners. Residual stresses may significantly influence the stress intensity factor (SIF) values and fatigue crack growth rate. A total SIF value, K_{tot}, is contributed by the part due to the applied load, K_{app}, and by the part due to weld residual stresses, K_{res}, as given by equation (4):

$$K_{tot} = K_{appl} + K_{res} \tag{4}$$

The so-called residual stress intensity factor, K_{res}, is required in the prediction of fatigue crack growth rates. The considered analysis method is based on the superposition rule of linear elastic fracture mechanics (LEFM). The finite element method (FEM) has been widely employed for calculating SIFs. For evaluating K_{res}, it is important to input correct initial stress conditions to numerical models in order to characterize residual stresses [22, 25]. In the FE software package ANSYS [26] the command INISTATE is used for defining the initial stress conditions.

4.1. Specimen's geometry and loading conditions

Fatigue tests with constant stress range and frequency were carried out on a stiffened panel specimen with a central crack, [23]. The specimen geometry is shown in Figure 4. The material properties of the used mild steel for welding are given in Table 1. Table 2 shows the fatigue test conditions applied in the experiment. The cross sectional area of the intact section, and the average stress range away from the notch, are denoted as, A_o and $\Delta\sigma_o$, respectively. The force range, and the stress ratio are denoted by $\Delta F = F_{max} - F_{min}$, and $R = F_{min}/F_{max}$, respectively. The average applied stress range was $\Delta\sigma_o$ = 80MPa. The initial notch length was $2a$ = 8mm and the loading frequency was 3 Hz.

Table 1. Material properties

E – Young's modulus	206 000 MPa
ν - Poisson's coefficient	0.3
σ_o – Yield strength	235 MPa

Table 2. Fatigue test conditions

A_o [mm^2]	ΔF [N]	$\Delta\sigma_o$ [MPa]	R
1200	96000	80	0,0204

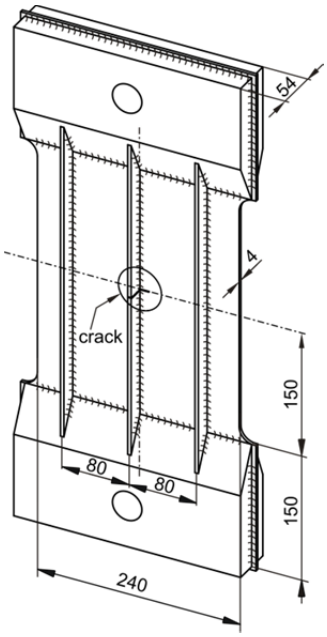

Figure 4. Stiffened panel specimen

4.2. Modeling of welding residual stresses in a stiffened panel by using FEM

In this study the distribution of welding residual stresses in a stiffened panel is taken into account in a similar manner as in the model developed by Dexter at. al. [22], and is shown in Figure 5. Dexter suggested the implementation of a rectangular shape of the residual stresses, which proved to give good results for the simulated fatigue life for such a type of welded stiffened panels.

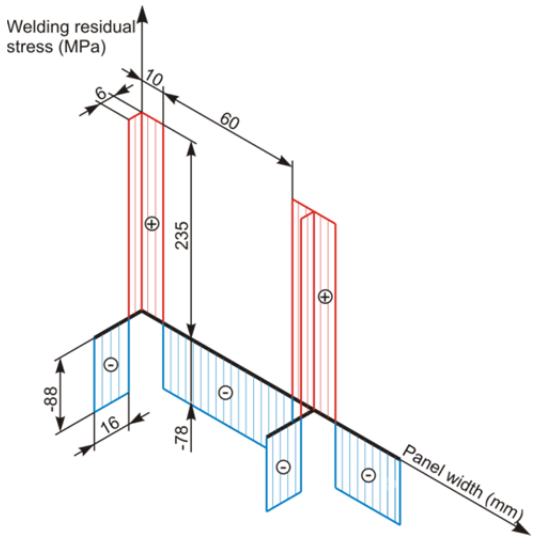

Figure 5. Welding residual stress distribution

To evaluate the SIF value contributed by the residual stresses, K_{res}, it is important to input correct initial stress conditions in the numerical model. In ANSYS software package the command INISTATE can be used to define initial stress conditions [26]. These initial stresses are equilibrated in the first analysis step. Due to the symmetry of specimen's geometry and loading conditions it was sufficient to model only one quarter of the specimen. Figure 6 shows welding residual stresses in the stiffened panel specimen obtained for the implemented stress distribution as given in Figure 5.

Figure 7 shows the σ_y stress component along a selected path in the crack line for the crack length a=4.7 mm, where in the model both, residual stresses and the loading stress range, $\Delta\sigma_o$ = 80MPa, are implemented. A higher stress concentration is observed in the crack tip region.

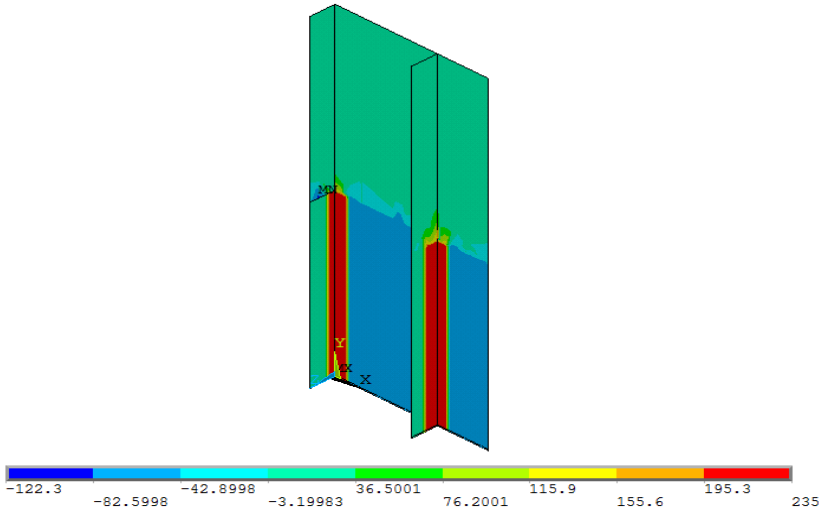

Figure 6. Welding residual stresses in the stiffened panel specimen

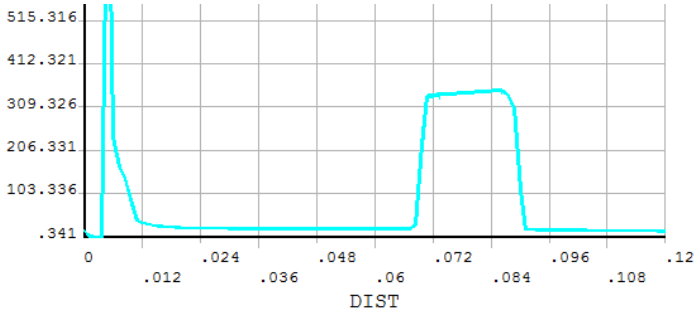

Figure 7. σ_y stress component along a selected path in the crack line

4.3. Stress intensity factors and fatigue crack growth rate

For evaluating SIFs by FEM, the crack tip displacements extrapolation method was implemented [26]. In the general post processing procedure, the "KCALC" command was used to calculate SIFs. The Mode I SIF values, K_I, are determined for a stiffened panel specimen for a loading stress range $\Delta\sigma_o$ = 80MPa, assuming the presence of residual stresses as described above. SIF values with respect to crack length a are given in Fig. 8. K_{app} represents the SIF values due to the applied stress range only, without residual stresses. K_{tot} represents the SIF values for the case when the residual stresses are taken into account along with the external loading stress range. It can be seen that residual stresses significantly increase K_{tot} values for shorter crack lengths, where tensile residual stresses prevail. Between the stiffeners residual stresses reduce the K_{tot} values.
Assuming material constants of a power law equation, C=5.05*10^{-11} and m=2.75 [27], fatigue life was simulated by integrating the power law equation as given by equation (5) (The units for ΔK and $\Delta a/\Delta N$ are [MPa $\cdot$m$^{1/2}$] and [m], respectively):

$$\frac{da}{dN} = C\left(\Delta K_{eff}\right)^m \tag{5}$$

The effective stress intensity range, ΔK_{eff}, was defined by Elber as $\Delta K_{eff} = K_{max} - K_{th}$, where K_{th} is a SIF threshold value below which no crack propagation occurs and K_{max} is the maximal SIF value in a loading cycle [24]. Assuming the stress ratio, $R = 0$, as applied in the experiment, the threshold SIF value for a mild steel, as used in the experiment, is taken as $K_{th} = 6.8$MPa, [28, 29]. For the two cases considered crack propagation life was obtained as shown in Figures 9 a) and b).

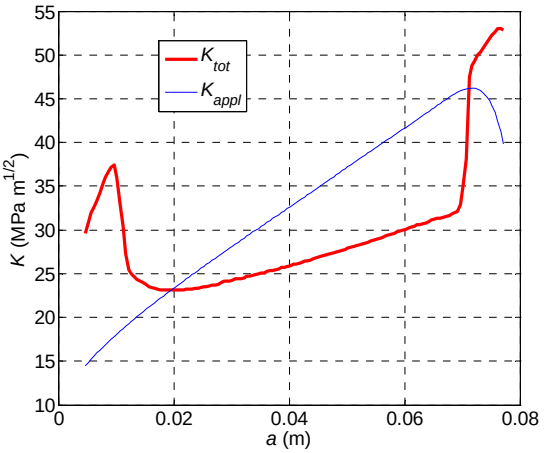

Figure 8. K_{tot} and K_{appl} values

The FE analysis for the stiffened panel specimens showed that high tensile residual stresses in the vicinity of a stiffener significantly increase K_{res} and K_{tot}, as shown in Figure 8. Correspondingly, the simulated crack growth rate was higher in this region, which is in good agreement with experimental results, as can be seen in Figure 9b. Compressive weld residual stresses decreased the total SIF value K_{tot}. The model which does not take account of welding residual stresses could not simulate high crack growth rates in the vicinity of the stiffener, as can be seen in Figure 9a.

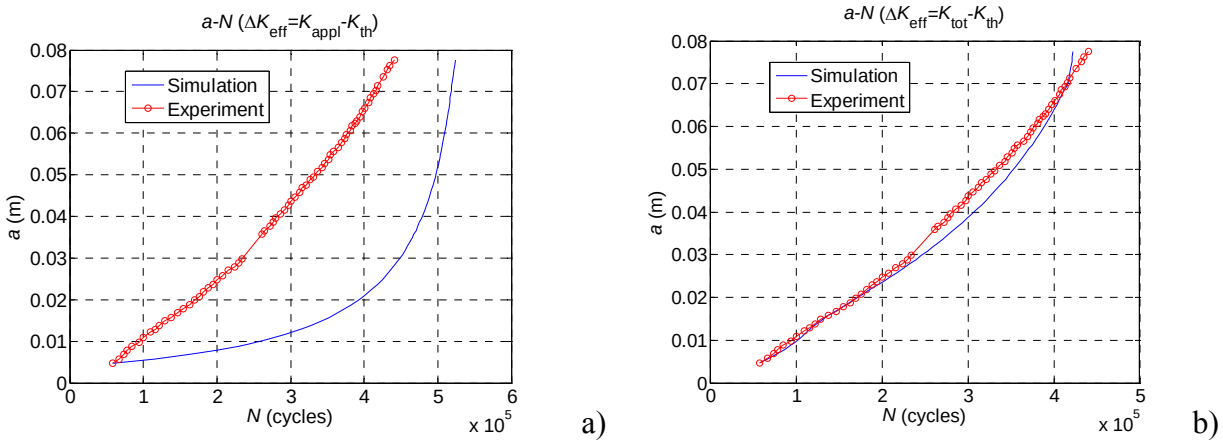

Figure 9. Fatigue crack growth life for the applied stress range $\Delta\sigma_o = 80$MPa : a) without residual stresses, b) including residual stresses

Fatigue crack growth simulation which takes into account the welding residual stresses provides thus better agreement with experimental results in terms of crack growth rate and total number of cycles. In conclusion, residual stresses in welded stiffened panels should be taken into account for a proper evaluation of SIFs and fatigue crack growth rates.

5. Conclusions

Simulation of cyclic loading to model fatigue is possible in MD. Already after very few cycles, essential changes in the system behavior were observed. Contrary to the first cycles, where reversible changes were dominant, not dissolving restructuring occurs in the sense of dislocations and remaining lattice defects or in other words, plasticity.
Numerical simulations of the fatigue crack initiation and growth of martensitic steel, based on modified Tanaka-Mura, was presented. A simulation model related to the micro-crack nucleation along slip bands was presented. Results obtained by using the proposed simulation model were compared to high cycle fatigue tests and showed reasonably good agreement.
Crack propagation simulation based on numerical integration of a power law equation, taking account of welding residual stresses, was implemented to welded stiffened panel specimens. The FE analysis of the stiffened panel specimens showed that high tensile residual stresses in the vicinity of a stiffener significantly increase K_{res} and K_{tot}. The simulated crack growth rate was higher in this region, which is in good agreement with experimental results. Compressive welding residual stresses decreased the total SIF value K_{tot}, and the crack growth rate between the two stiffeners. Residual stresses should thus be taken into account for a proper evaluation of SIFs and fatigue crack growth rates in welded stiffened panels.

Acknowledgements

This work was supported by the Deutsche Forschungsgemeinschaft (DFG) under Grant No. Schm 746/132-1. The support is gratefully acknowledged.

References

[1] J. Stadler, R. Mikulla, H.-R. Trebin, IMD: A software package for molecular dynamics studies on parallel computers, Int. J. Mod. Phys., 8 (1997) 1131.
[2] G. Bonny, R.C. Pasianot, N. Castin, L. Malerba, Ternary Fe-Cu-Ni many-body potential to model reactor pressure vessel steels: First validation by simulated thermal annealing, Phil. Mag., 89 (2009) 3531–3546.
[3] S. Grottel, G. Reina, C. Dachsbacher, T. Ertl, Coherent Culling and Shading for Large Molecular Dynamics Visualization, Computer Graphics Forum (Proceedings of EUROVIS 2010), 29(3) (2010) 953 – 962.
[4] A. Stukowski, V.V. Bulatov, A. Arsenlis, Automated identification and indexing of dislocations in crystal interfaces, Modelling Simul. Mater. Sci. Eng., 20 (2012) 085007.
[5] A. Stukowski, DXA user manual Version 1.3.4, (2010), http://dxa.ovito.org/README.txt
[6] S. Glodez, N. Jezernik, J. Kramberger and T. Lassen, Numerical modelling of fatigue crack initiation of martensitic steel, Advances in Engineering Software, 41(5) (2010) 823-829.
[7] WA. Wood, Fatigue in aircraft structures, Academic Press, New York, 1956.
[8] M.E. Fine, R.O. Ritchie, Fatigue-crack initiation and near-threshold crack growth. In: M. Meshii (Eds.), Fatigue and microstructure, Metals Park (OH): ASM, 1978, pp. 245–278.
[9] C. Laird, Mechanisms and theories of fatigue. In: M. Meshii (Eds.), Fatigue and microstructure. Metals Park (OH): ASM, 1978, pp. 149–203.
[10] M. Klesnil, P. Lukas, Fatigue of metallic materials, Elsevier, New York, 1980, pp. 57–80.
[11] H. Mughrabi, Rev Phys Appl, 23 (1988) 367–379.
[12] H. Mughrabi, In: K.S. Chan, P.K. Liaw, R.S. Bellows, T. Zogas, W.O. Soboyejo (Eds.), Fatigue: David L. Davidson symposium, Warrendale (PA): TMS, 2002, pp. 3–15.
[13] D.L. Davidson, K.S. Chan, Crystallography of fatigue crack initiation in Astrology at ambient

temperature. Acta Metall, 37(4) (1989) 1089–1097.
[14] Q. Y. Wang, C. Bathias, N. Kawagoishi, Q. Chen, Effect of inclusion on subsurface crack initiation and gigacycle fatigue strength. International Journal of Fatigue, 24(12) (2002) 1269-1274.
[15] Y. Murakami, T. Nomoto, T. Ueda, On the mechanism of fatigue failure in the superlong life regime ($N>10^7$ cycles). Part 1: influence of hydrogen trapped by inclusions. Fatigue Fract. Engng. Mater. Struct., 23(11) (2000) 893-902.
[16] K. Tanaka, T. Mura, A dislocation model for fatigue crack initiation. J. Appl. Mech., 48 (1981) 97–103.
[17] A. Brückner-Foit, X. Huang, Numerical simulation of micro-crack initiation of martensitic steel under fatigue loading. International Journal of Fatigue, 28(9) (2006) 963-971.
[18] N. Jezernik, J. Kramberger, T. Lassen, S. Glodez, Numerical modelling of fatigue crack initiation and growth of martensitic steels. Fatigue & Fracture of Engineering Materials & Structures, 33 (2010) 714–723.
[19] D. Broek, The Practical Use of Fracture Mechanics. Kluwer Academic Publishers, Dordrecht, The Netherlands, 1989.
[20] P. Paris, F. Erdogan, A critical analysis of crack propagation laws. Journal of Basic Engineering, 85 (1963) 528–534.
[21] R.J. Dexter, P.J. Pilarski, H.N. Mahmoud, Analysis of crack propagation in welded stiffened panels. International Journal of Fatigue, 25 (2003) 1169-1174.
[22] H.N. Mahmoud, R.J. Dexter, Propagation rate of large cracks in stiffened panels under tension loading. Marine Structures 18 (2005) 265-288.
[23] Y. Sumi, Ž. Božić, H. Iyama, Y. Kawamura, Multiple Fatigue Cracks Propagating in a Stiffened Panel. Journal of the Society of Naval Architects of Japan, 179 (1996) 407-412.
[24] W. Elber, The significance of fatigue crack closure. Damage tolerance in aircraft structures. ASTM STP 486. American Society for Testing & Materials; (1971) 230–242.
[25] R. Bao, X. Zhang, N. A. Yahaya, Evaluating stress intensity factors due to weld residual stresses by the weight function and finite element methods. Engineering Fracture Mechanics, 77 (2010) 2550–2566.
[26] Swanson Analysis System, Inc. ANSYS User's Manual Revision 11.0, 2009.
[27] Ž. Božić, H. Wolf, D. Semenski, Fatigue Growth of Multiple Cracks in Plates under Cyclic Tension. Transactions of FAMENA, 34(1) (2010) 1 – 12.
[28] Ž. Božić, S. Schmauder and M. Mlikota, Fatigue growth models for multiple long cracks in plates under cyclic tension based on ΔK_I, ΔJ-integral and $\Delta CTOD$ parameter. Key Engineering Materials, 488-489 (2012) 525-528.
[29] Y. Liu, S. Mahadevan, Threshold stress intensity factor and crack growth rate prediction under mixed-mode loading. Engineering Fracture Mechanics, 74, 2007, 332–345.